Advanced deflectometry methods for industrial application

Heejoo Choi, Hyukmo Kang, Yiyang Huang, Mina Yoo, Henry Quach, et al.

Heejoo Choi, Hyukmo Kang, Yiyang Huang, Mina Yoo, Henry Quach, John Kam, Daewook Kim, "Advanced deflectometry methods for industrial application," Proc. SPIE 12684, ODS 2023: Industrial Optical Devices and Systems, 1268407 (4 October 2023); doi: 10.1117/12.2678628

Event: SPIE Optical Engineering + Applications, 2023, San Diego, California, United States

Advanced deflectometry methods for industrial application

Heejoo Choi[a,b,*], Hyukmo Kang[a], Yiyang Huang[a], Mina Yoo[a], Henry Quach[d], John Kam[e], Daewook Kim[a,b,c]

[a]Wyant College of Optical Sciences, University of Arizona, 1630 E. University Blvd., Tucson, AZ 85721, USA
[b]Large Binocular Telescope Observatory, University of Arizona 933 N Cherry Ave., Tucson, AZ 85721, USA
[c]Department of Astronomy and Steward Observatory, University of Arizona, 933 N. Cherry Ave., Tucson, AZ 85721, USA
[d]ASML, 17075 Thornmint Court, San Diego, CA 92127, USA
[e]Microsoft, 1045 La Avenida St, Mountain View, CA 94043, USA

ABSTRACT

Deflectometry is a versatile optical testing tool used in various fields, from astronomy to industrial applications, due to its non-null testing capability which facilitates precise measurement despite challenging optical surfaces and system layout constraints. In this manuscript, we present novel variational advancements to traditional deflectometry, towards universal functionality and system friendliness.

Traditional dark-field illumination is an inspection technique that is sometimes used to detect particles on a specular surface. Problems arise in its repeatability, as an intensity-based measurement is vulnerably dependent on the testing conditions of time, limiting its ability to be used in automated fashion. The first advancement leverages phase algorithms commonly seen in deflectometry; by adding a secondary light source (normal to the surface) and modulating each source's intensity with a time-varying sinusoid. The phase-based information has a higher sensitivity to the light scattered from a defect producing a more robust computational image process method that is now insensitive to the environment. The second advancement is an alignment method to obtain lower-order shape. While deflectometry proves effective in measuring mid-to-high frequency surface shape, it faces challenges when assessing low-order shape measurements like power, astigmatism, and coma due to relative position and alignment error between the unit under test (UUT) and the deflectometry system. To avert the necessity of additional instruments like a coordinate measuring machine, laser trackers, or interferometers, we leveraged computational fiducials and sensitivity matrices to identify and address misalignments effectively.

With enhanced capabilities and system-friendly features, our advanced deflectometry techniques provide powerful options in optical testing. By addressing the challenges in low-order shape measurements and incorporating dark field testing, our approaches extend the potential of deflectometry as a valuable tool in optical metrology across a broad spectrum of industries and scientific endeavors.

Keywords: deflectometry, dark field illumination, alignment, optical testing.

1. INTRODUCTION

The fabrication of semiconductors, display panels and optics demands high-quality production at scale, driving manufacturers to adopt Automatic Optical Inspection (AOI) processes for defect detection where has a benefit of 1) non-contact inspection, 2) quick and wide searching profile and 3) intuitive test results to understand defects. However, AOI encounters challenges in identifying small defects over large, freeform surfaces, such as those encountered in lithography processes for semiconductors and display panels and freeform optics fabrication and testing.

*hchoi@optics.arizona.edu

ODS 2023: Industrial Optical Devices and Systems, edited by Ryuichi Katayama,
Yuzuru Takashima, Proc. of SPIE Vol. 12684, 1268407
· doi: 10.1117/12.2678628

Deflectometry is a well-known optical testing method as an appealing solution with its broad dynamic slope-measuring range and ability to assess various optical surfaces without null optics. However, precise calibration and alignment are crucial for accurate surface slope measurements in deflectometry systems. The extremely high frequency information (e.g., scratch, dust and contamination) on the surface is limited by resolution of typical imaging systems. We have developed supplemental advancements to resolve the issues of detecting particle and contamination of the unit under fabrication (UUF), and the low order shapes of the UUF which are challenging in general deflectometry.

2. PRINCIPAL

2.1 Modulated dark field illumination

We developed a technique that fuses dark field illumination and deflectometry. Dark field illumination, known for its simplicity and effectiveness in biological sample microscopy, is adapted to detect particles on substrates and masks in semiconductor manufacturing[1,2]. Our methods novelty relies on capturing differences in phase, outperforming traditional intensity-based measurements which are susceptible to noise and varying conditions.

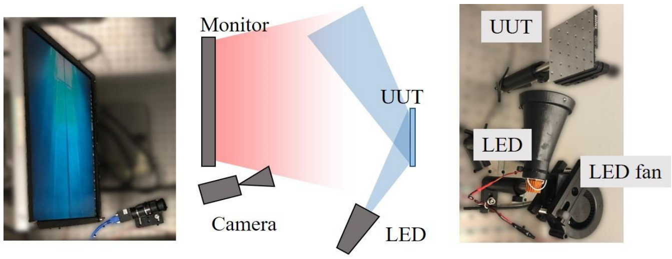

Figure. 1 System layout for modulated dark field illumination. The LED and monitor provide temporally separated illumination[3].

The system uses two light sources; a monitor normal to the surface of the unit under test and an external LED whose incidence grazes the surface. The intensity of each source is modulated by time-varying sinusoids, ensuring that the grazing LED and the monitor produce signals that are out of phase with respect to one another. At each phase step in sinusoid driving illumination an image is taken. This image stack along with image processing allows for the creation of a phase-index, where each pixel is assigned a phase value rather than an intensity value, cleanly distinguishing particles and background with specific values. This phase information leads to stable results, even with low particle intensity values, as the calculated phases remain consistent for each particle (see Fig. 2(a)). Thus, a simple threshold criterion can be used to achieve reliable and repeatable results without human intervention.

Furthermore, the phase-based approach is advantageous when dealing with intensity-sensitive marks, such as mask patterns on the UUT. While the traditional intensity difference map displays such marks, they do not appear in the phase map (as demonstrated in Fig. 2(b)). This feature enhances the accuracy and specificity of defect detection, providing a comprehensive and effective inspection process.

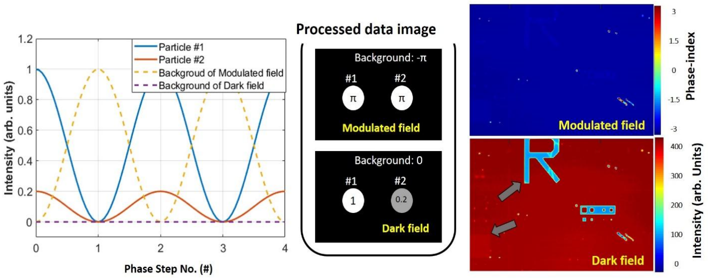

(a) (b)

Figure 2. The advantage of MF (Modulated Dark Field) calculations[3]. (a) Phase trend for each scattering and total reflection object and the schematic processed data image. The MF method demonstrates consistent phase-index differences for different intensity variation cases (Particles #1 and #2). (b) Measured data using MF (above) and dark field (below) methods on a sample with mask patterns (Grey arrows). The MF method provided uniform phase contrast to both background and mask patterns, effectively isolating particle signals. In contrast, the intensity-based dark field measurement is affected by the reflectance from mask patterns.

2.2 Recovering misalignment of deflectometry

We present an innovative alignment algorithm for precise alignment of deflectometry systems. Our method displays a uniform distribution of fiducial grid spots at the deflectometry camera image plane and fits the resulting pattern to a systematic vector polynomial set, the G and C[4,5] polynomials. The result of this inversely-calculated computational fiducial, is the qualitative assessment for alignment of non-null testing scenarios.

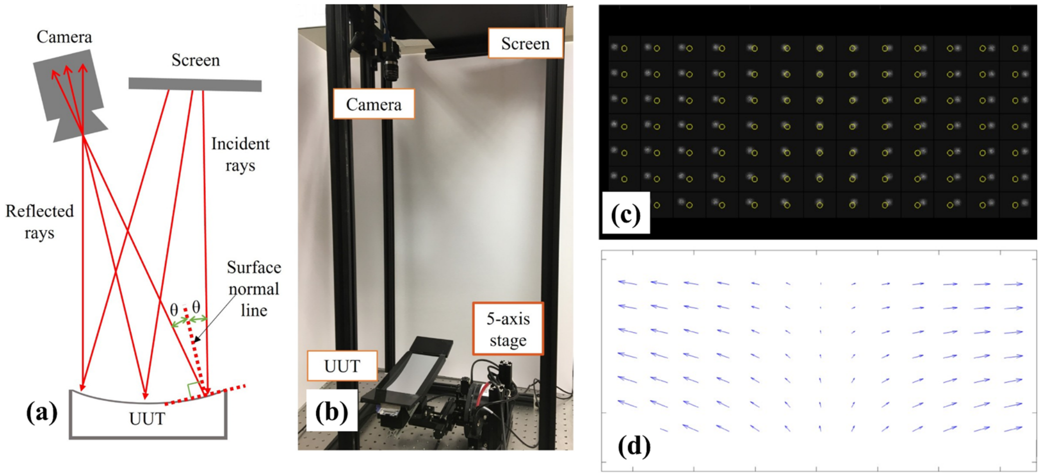

Figure 3. (a) Schematic optical layout of deflectometry setup[6]. The computational fiducial grid is displayed on the screen and the camera obtains its image through the UUT reflection. (b) Actual experimental setup of deflectometry.
(c and d) Simulated images for computational fiducial pattern process. (c) Measured image of fiducial pattern at the camera detector plane. White dots are actual measured patterns and yellow circles are superimposed fiducial positions from ideal model.
(d) Vector map drawn from computational yellow circles to measured white dots, which are updated real-time.

To assist in the alignment of the deflectometry setup, we employ a computational fiducial pattern generated using the deflectometry ray tracing simulator [6]. This pattern maps a grid dot image onto the camera detector and is calculated based on model geometry ray trace. In Fig. 3 (c), the yellow circles represent the locations of the fiducial for a perfectly aligned system, while the recorded white dots indicate their observed locations through the UUT. Each dot is represented as a 2D Gaussian shape to reduce position determination ambiguity in centroiding calculation. Any deviation from the fiducial points indicates an inconsistency in the optical layout between the model and the experimental setup. The use of a rectangular grid dot pattern is preferable as it allows for the utilization of G and C polynomial sets. The computational fiducial pattern and its alignment algorithm play a crucial role in ensuring the accuracy and reliability of the deflectometry measurements. The fiducial dot pattern can be used to systematically quantify the misalignment status when it is associated with vector polynomials. As misalignments shift the image of the fiducial dots from their reference points, we can connect corresponding dots from their referenced position to their perturbed position to make vectors [Fig. 3 (d)].

3. EXPERIMENTAL RESULT

3.1 Modulated dark field illumination results

We carefully surveyed the phase difference and initial values for both light sources. A $-\pi/4$ and $+\pi/4$ are chosen for screen and LED, respectively. We used an off-the-shelf monitor (Dell 1097FP) and camera (Pointgrey, FL3-U3-13Y3M-C), as well as a three-point emitting LED (Cree LEDs, XHP 35) driven by an Arduino controller to produce the required modulated signal. The camera was placed 55 cm from the sample UUT, which was the Al-coated mirror, and under these conditions, a single detector pixel occupied an area of ~80 × 80 µm on the sample. To create a constant reference sample, we sprayed a clean surface with particles of a known size. A polycrystalline particle spray (Struers, DP-Spray P 35 µm) was used to deposit equal-sized particles (~35 µm) on the surface of the Al-coated UUT.

We repeated the test for both MF and traditional dark field test 10 times and checked the probability of the defect detection using home made AOI algorithm. When implementing the traditional dark field approach, even if a threshold value is carefully chosen for one trial, fluctuations between trials may change the intensity distribution. The green error bars in Fig. 4 (left) illustrate the fluctuations in the intensity distribution over the 10 trials. The top histogram in Fig. 4(left) clearly demonstrates the additional stability that the MF approach offers over the intensity-based dark field results (left, below), indicating a high-fidelity method. In other words, the modulated dark field phasing detection enables an enhanced robustness of the AOI method against random noise in the actual measurement signal. However, we also acknowledge that this does not mean 100% immunity to such noise. Just like other systems with uncertainties, there is still a chance, albeit small, for false-positives and missed particles depending on the actual magnitude of the noise and the intrinsic errors of the built system.

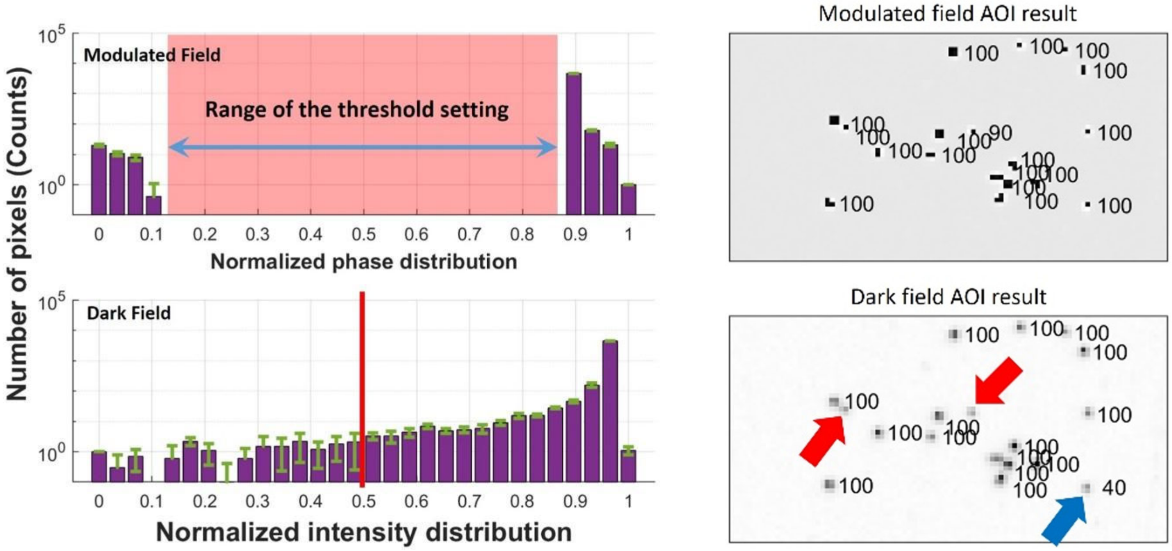

Figure 4. Comparison of particle detection measurement results from the different methodologies[3]. (left) Histogram of the pixel value distribution, showing the phase-index (top) and intensity (bottom) from all pixels. The possible range of threshold settings is shown in the red zone. (right) AOI defect detection percentage (%) results for MF (above) and dark field (bottom) measurements. In the case of a fixed threshold value, the dark field method failed to detect three particles, two completely (red arrow) and one 60% of the time (blue arrow), whereas the modulated field AOI was able to detect all one particle, which was still detected 90% of the time.

3.2 Computational vector fiducial alignment

In total, ten alignment experiments were executed, and their results are displayed in Fig. 5. The root mean square (RMS) vector length effectively met the predefined criteria, indicating a successful overall alignment process. However, the remaining misalignments showed variations among different degrees of freedom. Notably, Dy, Dz, and Tz exhibited excellent convergence and alignment, demonstrating their robustness in the alignment procedure. Conversely, while Dx and Ty also achieved convergence, they displayed relatively larger persistent errors.

The primary challenge with Dx and Ty lies in their production of similar fiducial motion, resulting in difficulty distinguishing between them in vector space. Consequently, accurate resolution of the misalignments for these particular degrees of freedom necessitates additional attention and possible refinement of the alignment methodology. Nevertheless, the alignment experiments yielded promising outcomes overall, with several degrees of freedom successfully and precisely converging. This improvement in alignment greatly enhances the overall accuracy and reliability of the deflectometry system, reinforcing its potential as a powerful tool for metrology applications.

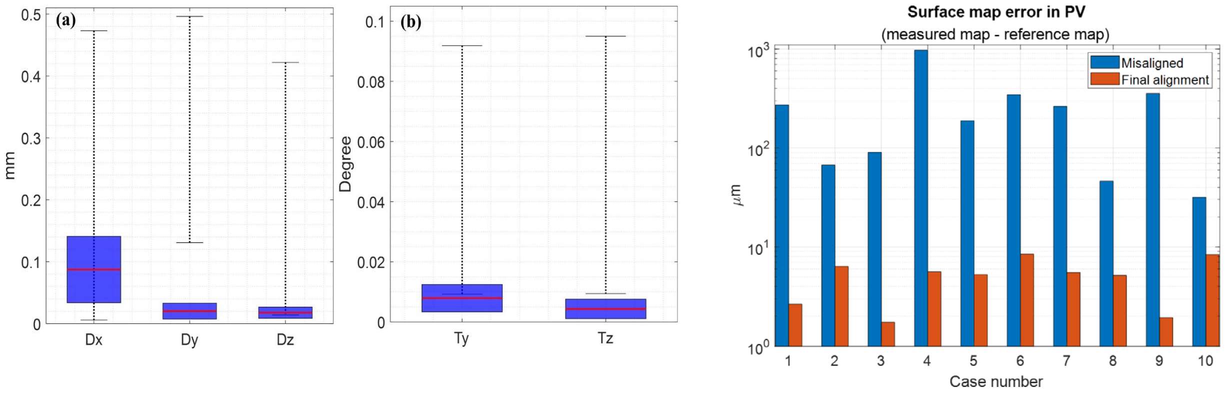

Figure 5. Alignment experimental results. (left) Residual error in each degree of freedom after the automatic alignment process from ten random perturbations. Dotted vertical lines indicate the initial random perturbation range, red lines represent the mean values of remaining errors after alignment, and blue boxes represent the standard deviations for the ten cases. (right) The optical testing error comparison for before and after. The blue box presents the wavefront error resulting from random perturbations of the UUT, and the red box presents the residual wavefront error after the alignment process using vector fiducials.

We want to emphasize that the accuracy of the alignment status estimation was primarily limited by the precision of the motorized stage, rather than the algorithm itself, as long as the misalignment remains within a linear range of sensitivity. In the G and C polynomial fitting results, we observed distinct behaviors for translation and tilt motion in higher-order coefficients, which were relatively small in magnitude. Consequently, enhancing the accuracy of the alignment can be achieved by obtaining more vector data over higher G/C orders or utilizing higher resolution cameras in the deflectometry system to ensure more accurate spot measurement. To evaluate the alignment results, we compared the peak-to-valley (PV) of the subtracted map between an ideal surface map and the surface map before/after alignment. The reference was the surface map measured at the home position of the motorized stage. As a result, the difference map demonstrates both the alignment loop's capability to bring the UUT back to its original position and the repeatability of optical testing. The PV surface map error attributed to residual misalignment was consistently less than 8.4 µm in all ten experiments (Fig. 5, right). This outcome affirms that the proposed algorithm can effectively guide the deflectometry system alignment to secure repeatability in optical testing, eliminating the need for additional alignment devices. In essence, this computational alignment serves as the deflectometry counterpart of the alignment mode commonly used in interferometry setups.

4. CONCLUSION

We have developed a reliable Automatic Optical Inspection (AOI) method for defect and contamination test by integrating dark field illumination with methods from deflectometry. This phase-based approach enables the detection of small defects with stable results, even at low recorded particle intensity values. The combination of dark field illumination and deflectometry methods also offers significant advantages in freeform metrology, enhancing the precision of surface slope measurements.

Our proposed alignment algorithm using a computational fiducial has demonstrated promising results in guiding the deflectometry system to achieve accurate convergence. This advancement simplifies the metrology process without additional devices, making deflectometry a more accessible and practical option for various optical surface measurements in industrial applications.

The application of our AOI and alignment methodologies in semiconductor and display panel manufacturing industries offers reliable and efficient tools for defect detection and product quality assurance. The automation and accuracy provided enable mass production of high-quality products, improving competitiveness and profit margins with minimum hardware requirements. Looking ahead, we aim to optimize and expand the applications of our techniques to further enhance measurement precision and address a broader range of optical surfaces and systems. Our research contributes to advancing optical testing and metrology, driving innovations in precision engineering, and the development of cutting-edge technologies with broader societal impact.

REFERENCES

[1] S. H. Gage, “Modern dark-field microscopy and the history of its development,” Transactions of the American Microscopical Society 39(2), 95-141 (1920).

[2] M. Feldman and O. W. Lynn, “Inspection system utilizing dark-field illumination,” U.S. Patent 4,595,289 (Jun 17, 1986).

[3] Heejoo Choi, John Mineo Kam, Joel David Berkson, Logan Rodriguez Graves, Dae Wook Kim, "Modulated dark-field phasing detection for automatic optical inspection," Opt. Eng. 58(9) 092603 (26 March 2019)

[4] M. Aftab, J. H. Burge, G. A. Smith, L. Graves, C.-J. Oh, and D. W. Kim, Int. J. Precis. Eng. Manuf. Technol. 6, 255 (2019).

[5] M. Aftab, L. R. Graves, J. H. Burge, G. A. Smith, C. J. Oh, and D. W. Kim, Opt. Eng. 58, 095105 (2019).

[6] Kang, Hyukmo, Henry Quach, Joel Berkson, Maham Aftab, George Smith, Heejoo Choi, and Daewook Kim. "Computational vector fiducial for deflectometry system alignment." Optics Letters 46, no. 22 (2021): 5571-5574.